A simple method to describe stress path dependency of plastic flow

Teruo Nakai[1] and H.Md. Shahin[2]

[1] Geo- Research Institute, Nagoya Office, Nagoya, Japan.
[2] Islamic University of Technology, Board Bazar, Gazipur 1704, Bangladesh.

ABSTRACT

According to the classic theory of plasticity, the direction of plastic flow (direction of plastic strain increments) is independent of the direction of stress increments. This means that the stress-dilatancy relation (stress ratio-plastic strain increment ratio relation) is not influenced by the stress path. However, it is experimentally pointed out that the stress-dilatancy relation of soils depends on the stress path except for the stress condition near or at failure. In the present research, we have proposed a method of expressing the stress path dependency of the direction of plastic strain increment in a simple and rational way without increasing the number of parameters, which is applicable from normally consolidated soil to structured soil. The validity and necessity of the proposed method are clarified through analysis of element tests and deformation analysis of embankment ground.

Keywords: constitutive model, flow rule, deformation characteristics

1 INTRODUCTION

To describe the stress path dependency of plastic flow, usually double hardening theory and tangential plasticity theory are employed. However, in these theories, plural sets of yield functions and hardening parameters and additional coefficients of tangential plasticity are necessary which makes constitutive model complex and needs more material parameters.

One of authors tried to explain such behavior by splitting the plastic strain increment into two components – one is the plastic strain increment which satisfies the associated flow rule and the other is the isotropic plastic strain increment with the increase of mean stress - despite one set of yield function and others (Nakai and Hinokio 2004). However, this formulation was not obtained in a robust fashion. In the present paper, the authors present alternative and rational formulation of splitting strain increment. Here, although the plastic strain is split into two components in the same way as before, the present formulation is done where the combined plastic volumetric strain, which is the hardening parameter, is always the same as that of the model obeying associated flow rule. As a result, the loading condition remains same as that of the model obeying associated flow rule.

2 STRESS PATH DEPENDENCY OF THE DIRECTION OF PLASTIC FLOW IN SOIL

Fig.1 shows the observed relations between stress ratio and strain increment ratio of triaxial compression and extension tests on normally consolidated Fujinomori clay under various stress paths (constant mean principal stress (p), constant major principal stress (σ_1), constant minor principal stress (σ_3), and constant principal stress ratio ($R=\sigma_1/\sigma_3$). Diagram (a) shows the arrangement based on the stress parameters (p, q) and the strain increment parameters ($d\varepsilon_v$, $d\varepsilon_d$), which are commonly used in Cam clay type model. Diagram (b) shows the arrangement based on the stress parameters (t_S, t_N) and the strain increment parameters ($d\varepsilon_N$, $d\varepsilon_S$) based on the t_{ij} concept (Nakai and Mihara 1984). It can be seen form diagram (a) that the arrangement using ordinary stress and strain increment parameters not only depends on compression or extension, but also greatly influenced by the stress path. On the other hand, in the arrangement based on t_{ij} concept, though there is no difference between compression and extension, the strain increment ratio still depends on the stress paths except near and at peak stress. Here, although it is arranged by total strain, it does not change much, even if it is arranged only by plastic strain. In Fig.1, the strain increment ratio deviates leftward when the mean stress increases (σ_3=const. and $R=\sigma_1/\sigma_3$=const.), and the strain

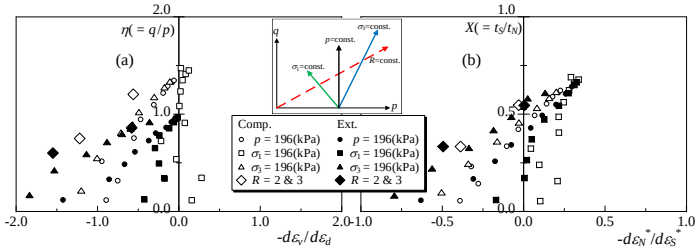

Fig. 1. Observed stress ratio – strain increment relation of normally consolidated clay.

increment ratio deviates rightward when the mean stress decreases (σ_1=const.). Here, deviating leftward means that the occurrence of deviatoric strain is smaller, and deviating rightward means that the occurrence of deviatoric strain is larger for the same volume change. This stress path dependency was reported on sand as well (Tatsuoka 1978)

Fig.2 shows the relation between the stress ratio and the plastic strain increment ratio (stress-dilatancy relation) of (a) Original and Modified Cam clay model, and (b) Subloading t_{ij} model (AF) (Nakai and Hinokio 2004) satisfying the associated flow rule in t_{ij} space, respectively. In the model with stress parameters (p, q) like the Cam clay model, the relation of diagram (a) is assumed to be determined uniquely regardless of the intermediate principal stress and stress path. In the Subloading t_{ij} model obeying the associated flow rule (AF), it is assumed that the relation in diagram (b) holds uniqueness regardless of the intermediate principal stress and the stress path.

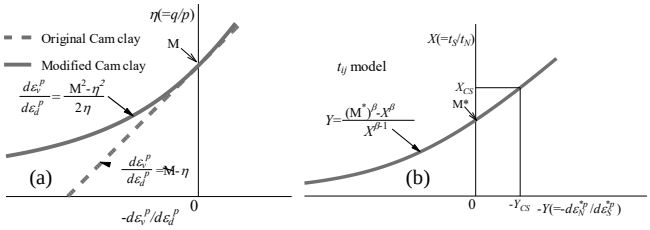

Fig. 2 Stress-dilatancy (a) Cam clay model, (b) t_{ij} model

3 MODELING OF STRESS PATH DEPENDENCY ON THE DIRECTION OF STRAIN INCREMENT

To describe the stress path dependency in general three dimensional conditions, Subloading t_{ij} model (Nakai et al. 2011; Nakai 2012) obeying the associated flow rule (AF) is extended here. Fig. 3 shows the yield surface of Subloading t_{ij} model, which considers not only the intermediate principal stress but also density and bonding, is expressed by the following equation as the function of the mean stress t_N and the stress ratio X=t_S/t_N.

$$f = F - H - \frac{1}{\lambda-\kappa}(\rho_0 - \rho) = 0,$$

$$\text{where} \quad F = \ln\frac{t_{N1}}{t_{N0}} = \ln\frac{t_N}{t_{N0}} + \varsigma(X), \quad \varsigma(X) = \frac{1}{\beta}\left(\frac{X}{M^*}\right)^{\beta} \tag{1}$$

$$H = \frac{(-\Delta e)^p}{\lambda-\kappa} = \frac{1+e_0}{\lambda-\kappa}\varepsilon_v^p$$

In Eq.(1), e_0 is the initial void ratio, λ is the compression index, κ is the swelling index, $\varsigma(X)$ is the function of the stress ratio X and determines the shape of the yield surface in Fig. 3(a) (β is the corresponding parameter), and M^* is determined from the stress ratio R_{CS} at the critical state. In addition, as shown in Fig. 3(b), ρ represents the difference between the current void ratio e and the void ratio e_{NC} on the normal consolidation line (NCL) of the same stress state, and it is a state variable representing the density of the material, ρ_0 is its initial value. The evolution rule of ρ with the development of plastic deformation for structured soils can be determined not only by the state variable ρ related to density but also by the state variable ω representing the bonding effect with an imaginary increase of density, and the value of the state variable ω has an additional effect on the degradation of ρ (Nakai et al. 2011; Nakai 2012).

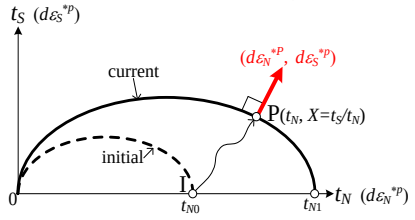

(a) Yield surface on (t_N, t_S) plane

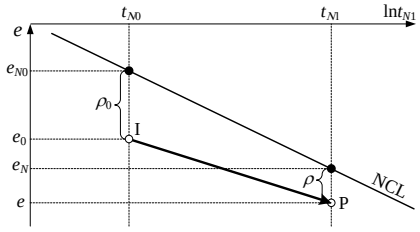

(b) e - lnt_{N1} curve

Fig. 3 Explanation of Subloading t_{ij} model

Using the consistency condition (df=0) and the flow rule (associated flow rule in t_{ij} space: $d\varepsilon_{ij}^p = \Lambda\cdot(\partial F/\partial t_{ij})$), the plastic strain increment and the plastic volumetric strain (increment of hardening parameter) are given by the following equations.

$$d\varepsilon_{ij}^p = \Lambda\frac{\partial F}{\partial t_{ij}} = \frac{dF}{\dfrac{1+e_0}{\lambda-\kappa}\left\{\dfrac{\partial F}{\partial t_{kk}} + \sqrt{3}\dfrac{G+Q}{t_N}\right\}}\frac{\partial F}{\partial t_{ij}} = \frac{dF}{h^p}\frac{\partial F}{\partial t_{ij}} \tag{2}$$

$$\left(\text{where,}\ \ h^p = \frac{1+e_0}{\lambda-\kappa}\left\{\frac{\partial F}{\partial t_{kk}} + \sqrt{3}\frac{G+Q}{t_N}\right\}\right)$$

$$d\varepsilon_v^p = d\varepsilon_{mm}^p = \Lambda\frac{\partial F}{\partial t_{mm}} = \frac{dF}{h^p}\frac{\partial F}{\partial t_{mm}} \tag{3}$$

Now, the plastic volume strain, which is the increment of handing parameter, of (AF) model is transformed by adding and subtracting the same terms.

$$d\varepsilon_v^p = \frac{dF}{h^p}\frac{\partial F}{\partial t_{mm}} = \frac{dF}{h^p}\frac{\partial F}{\partial t_{mm}} - \left\langle\frac{\partial F}{\partial t_{kk}}\frac{t_N}{\sqrt{3}}\right\rangle^2 A\frac{dt_N}{t_N}\frac{\partial F/\partial t_{mm}}{\partial F/\partial t_{kk}} + \left\langle\frac{\partial F}{\partial t_{kk}}\frac{t_N}{\sqrt{3}}\right\rangle^2 A\frac{dt_N}{t_N}\frac{\delta_{mm}}{3} \tag{4}$$

($\partial F/\partial t_{mm}/\partial F/\partial t_{kk}$ =1; $\delta_{mm}/3$ =1)

Then, plastic strain increment is expressed as follows by changing indices mm to ij :

$$d\varepsilon_{ij}^{p}=\underbrace{\left\{\frac{dF}{h^{p}}-\left\langle\frac{\partial F}{\partial t_{kk}}\frac{t_N}{\sqrt{3}}\right\rangle A\frac{dt_N}{\sqrt{3}}\right\}\frac{\partial F}{\partial t_{ij}}}_{\text{(AF)}}+\underbrace{\left\langle\frac{\partial F}{\partial t_{kk}}\frac{t_N}{\sqrt{3}}\right\rangle^{2}A\frac{dt_N}{t_N}\frac{\delta_{ij}}{3}}_{\text{(IC)}}=d\varepsilon_{ij}^{p(AF)}+d\varepsilon_{ij}^{p(IC)} \tag{5}$$

Here, as shown in Fig. 4, $\left\langle \partial F/\partial t_{kk}\cdot t_N/\sqrt{3}\right\rangle$ is a positive decreasing function of stress ratio X, which is 1 at X=0 (isotropic stress), because $\partial F/\partial t_{kk}\big|_{X=0}=\sqrt{3}/t_N$. Also, "$A$" is the positive coefficient which corresponds to the inverse of plastic modulus h_p under isotropic compression.

$$A=\frac{1}{h^{p(IC)}}=\frac{1}{\frac{1+e_0}{\lambda-\kappa}\{1+\langle G+Q\rangle\}} \tag{6}$$

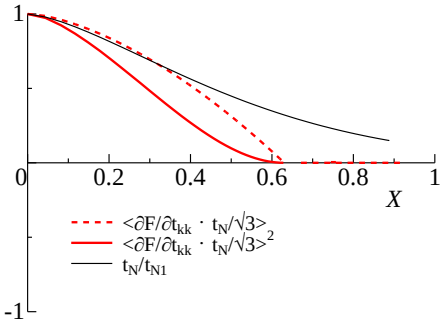

Fig. 4 Function determining isotropic compression (IC) component

It can be seen from the above formulation that the plastic strain increment is isotropic component alone under isotropic compression, and isotropic component becomes relatively small with increasing stress ratio X.

Functions G and Q in Eqs. (2) and (6) are the monotonically increasing functions of density (ρ) and bonding (ω), and the evolution rules of ρ and ω can be depicted as.

$$d\rho=-(1+e_0)\sqrt{3}\frac{G+Q}{t_N}\Lambda,\quad d\omega=-(1+e_0)\sqrt{3}\frac{Q}{t_N}\Lambda \tag{7}$$
$$\left(e.g.,\ G=a\rho^{2},\ \ Q=b\omega\right)$$

Fig. 5 explains how yield surface and plastic strains are generated in the (t_N, t_S) space. For example, when the stress changes from the current stress (point A) to the point B (dt_N <0) or when it changes to the point C (dt_N > 0), the plastic strain increment is obtained from the sum of the associated flow rule component and the isotropic compression component, regardless of an increase or decrease of t_N. Furthermore, if the succeeding loading surfaces are same in both points B and C, the generated plastic volumetric strain for this part will also be the same, and it is consistent with the associated flow rule model. As a result, the loading condition can also be the same as that of the associated flow rule (AF) model, as shown by the following equation.

$$\begin{cases} d\varepsilon_{ij}^{p}=d\varepsilon_{ij}^{p(AF)}+d\varepsilon_{ij}^{p(IC)}\neq 0 & \text{if } \Lambda=\dfrac{dF}{h^{p}}\geq 0\\ d\varepsilon_{ij}^{p}=0 & \text{otherwise}\end{cases} \tag{9}$$

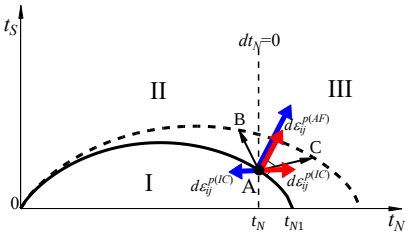

Fig. 5 Direction of plastic strain increment

The total strain increment can be determined by adding the elastic strain increment obtained from the nonlinear elastic equation (using swelling index κ and Poisson's ratio ν) to the plastic strain increment of Eq. (5).

4 SIMULATION OF ELEMENT TESTS

Analyses are done using the same material parameters listed in Table 1. Here, ω_0 and b are not necessary for non-structured soil.

Table1 Parameter of Fujinomori clay

λ	0.104	
κ	0.010	
N (e_N at p = 98kPa)	0.83	Same parameters as Cam clay model
$R_{CS}=(\sigma_1/\sigma_3)_{CS\,(comp.)}$	3.5	
ν_e	0.2	
β	1.5	Shape of yield surface (same as original Cam clay if β = 1)
a	290 (≈500/√3)	Influence of density and confining pressure
ω_0	0.0 (no bonding) 0.4 (with bonding)	Influence of bonding
b	23 (≈40/√3)	

Fig. 6 shows the computed results corresponding to the observed values in Fig.1(b), which shows good agreement between the computed and observed results. The thick solid gray line shows the relation in Fig. 2(b).

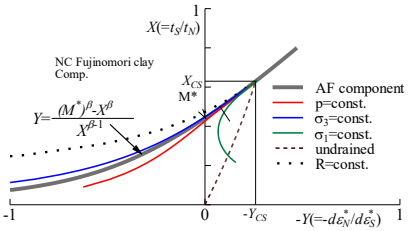

Fig. 6 Computed stress ratio – strain increment ratio relation

Fig.7 shows *K*o values with axial strain obtained from different model. It is loaded from an over-consolidated state (OCR=2.9) which finally reaches to the normally consolidation state. *K*o value of the Original Cam clay model (thin dotted line) is large, and for the Modified model (thin solid line) still it is about 0.6. Also, Subloading t_{ij} model obeying the associated flow rule (thick broken line; t_{ij}(AF)) over predict K_0 value. On the other hand, K_0 value predicted by Subloading t_{ij} model (AF+IC; Alt.), which considers the stress path dependency, is around 0.5 in normally consolidated state.

Fig. 8 shows the computed results of isotropic compression and undrained shear tests on structured clay. Shear tests are started from the ○ marks in diagram (a) at p_0=98kPa, 1440kPa. The isotropic compression curves are the same regardless whether the (IC) component is considered or not. However, in the analysis without considering the (IC) component, the deviatoric strain for undrain shear at p_o=1400kPa is significantly smaller.

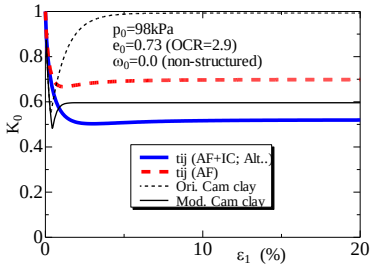

Fig. 7 Computed K_0 by four kinds of models

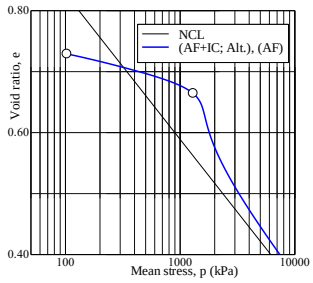

(a) Isotropic consolidation curves

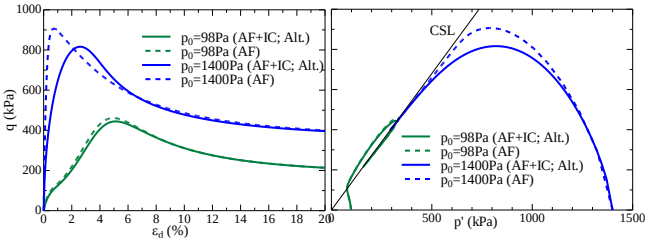

(b) Effective stress path (c) Stress-strain relation

Fig. 8 Results of consolidation test and undrained triaxial tests

5 SIMULATION OF EMBANKMENT GROUND

Fig.9 illustrates the layout of the embankment to be analyzed using associated flow rule (AF) and the model considering the dependency of the stress path (AF+IC; Alt.). The clayey ground without bonding is made by simulating self-weight consolidation. Fig. 10 shows the surface settlement profiles and lateral displacement below the toe of the embankment immediately after completion of the embankment and after 1000 days (after complete dissipation of the excess pore water pressure of the ground). It is found that just after soil fill, there is no significant difference of the results (surface settlement and lateral displacement) obtained from both models. However, settlement right below the embankment is a bit smaller in the subsequent process of dissipating the pore water pressure in the (AF+IC; Alt.) model, though, there is no big difference around the toe of the embankment in both models. However, looking at the lateral displacements, in the (AF) model, the lateral displacement increases during the pore water pressure dissipation. In the (AF+IC; Alt.) model, though lateral displacement increases slightly at the lower part of the ground, hardly any change is seen in the lateral displacement at the upper part of the ground during the dissipation of the excess pore water pressure (rather a return to the embankment side is seen). The trend of the results corresponds to that commonly observed at the site of clayey ground. Usually, in deformation analysis of embankment ground, the amount of settlement is somewhat similar, but the amount of lateral displacement is always predicted excessively (particularly in the consolidation period), this is due to the path dependency of the direction of strain increment is not taken into consideration in constitutive models.

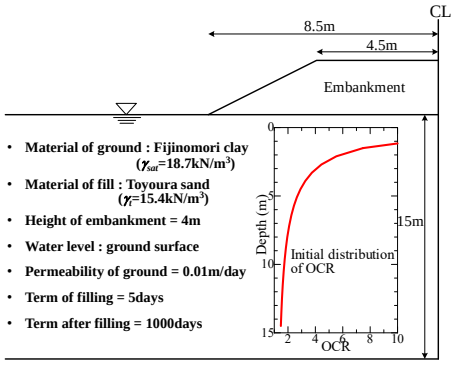

Fig. 9 Layout for the simulation of embankment

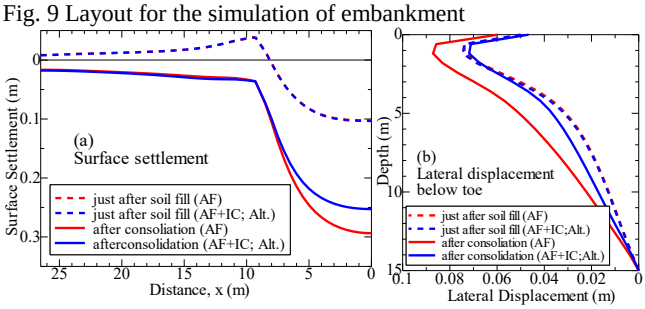

Fig. 10 Simulation results of the base ground of the embankment

6 CONCLUSIONS

Without increasing any material parameter, a method is proposed which can rationally explain the path dependency on the direction of strain increment which usually cannot be explained with an ordinary elastoplastic model. Moreover, its validity has been verified through element test and embankment analysis.

REFERENCES

Nakai, T. and Mihara, Y. (1984). A new mechanical quantity for soils and its application to elastoplastic constitutive models, Soils and Foundations, 24(2), 82-94.

Nakai, T. and Hinokio, M. (2004). A simple elastoplastic model for normally and over consolidated soils with unified material parameters, Soils and Foundations, 44(2), 53-70.

Nakai, T., Shahin, H.M., Kikumoto, M., Kyokawa, H., Zhang, F. and Farias, M.M. (2011). A simple and unified three-dimensional model to describe various characteristics of soils, Soils and Foundations, 51(6), 1149-1168.

Nakai, T. (2012). Constitutive Modeling of Geomaterials: Principles and Applications, CRC Press,. Boca Raton, London, New York.

Tatsuoka, F. (1978). Stress-strain behavior of an idealized granular material by simple elastoplastic theory, Proc. of U.S.-Japan Seminar on Continuum Mechanical Statistical Approaches of Granular Materials, Sendai, 301-32.